



ISSN: 0067-2904

Effect of Films Thickness on Structural and Optical Properties of Gold (Au) Thin Films Prepared by DC Magnetron Sputtering

Moatasim Amer*, Alaa Jabbar Ghazai

Physics Department, College of Science, Al-Nahrain University, Baghdad, Iraq

Received: 8/6/2021

Accepted: 20/8/2021

Published: 30/4/2022

Abstract

In this paper, the effect of films thickness on the structural and optical properties of gold (Au) thin films prepared by the DC sputtering method was studied. At three different deposition times, three samples of gold thin films of three different thicknesses (200,400, and 600 nm) were prepared. X-ray diffraction patterns, scanning electron microscopy (SEM), and atomic force microscopy (AFM) images, as well as optical spectroscopy, were used to characterize thin films. The crystalline structure of gold thin films was determined by the XRD pattern which showed to be cubic phase and polycrystalline in nature. The preferred orientation was (111) at 2θ equal 37.4. The effect of deposition time on the morphology of the deposited films was visualized with a scanning electron microscope (SEM) which showed a homogenous surface with nanoparticles with a diameter size of 50-100 nm. Changes in deposition time caused variations in roughness, thickness, and surface quality, as shown by AFM results. UV-Vis reflection spectroscopy was also used to investigate the optical properties of thin films.

Keywords: Gold, thin film, high reflectance, DC sputtering, optical properties, structural properties

تأثير سمك الغشاء على الخصائص التركيبية والبصرية لأغشية الذهب الرقيق المحضر بطريقة التريز

معتصم عامر*, علاء جبار

قسم الفيزياء، كلية العلوم، جامعة النهرين، بغداد، العراق

الخلاصة

في هذا البحث تم دراسة تأثير سمك الفيلم على الخصائص التركيبية والبصرية لغشاء الذهب الرقيق (Au) المحضر باستخدام طريقة التريز ذو التيار المستمر. في ثلاث اوقات ترسيب مختلفة، تم إنشاء ثلاث عينات من أغشية الذهب الرقيقة ذات اسماك مختلفة. تم استخدام أنماط حيود الأشعة السينية، والفحص المجهر الإلكتروني (SEM)، وصور مجهر القوة الذرية (AFM)، بالإضافة إلى التحليل الطيفي البصري، لتوصيف الأغشية الرقيقة. تم تحديد التركيب البلوري لأغشية الذهب الرقيقة باستخدام نمط XRD الذي كان طورًا مكعبًا ومتعدد البلورات. وأفضل متجه هو (111) عندما ضعف زاوية تساوي 37.4، تم تصوير تأثير معدل الترسيب على شكل الأغشية المترسبة باستخدام المجهر الإلكتروني الماسح (SEM) الذي أظهر سطحًا متجانسًا مع جسيمات نانوية بحجم قطر 50-100 نانومتر. تسببت التغييرات في وقت الترسيب في حدوث

*Email: moatasimamer@gmail.com

اختلافات في الخشونة والسمك وجودة السطح، كما هو موضح في نتائج AFM. كما تم استخدام التحليل الطيفي لانعكاس الأشعة فوق البنفسجية لفحص الخصائص البصرية للأغشية الرقيقة.

1. Introduction

Developing the approaches for obtaining nanostructures of noble metals with complete control over the shape of surface structures remains a major challenge. In fact, the real objective is to produce small objects with reproducibly matching the requirements of many applications[1]. The efficiency and behavior of a material can be affected by its surface properties. It is possible to modify and tune these surface properties to meet a specific demand for improved performance, and this has been done extensively in a variety of fields. Coating the surface with a thin film is one way to accomplish this[2]. Nano-crystalline thin solid films are currently generating a lot of interest in the scientific community, owing to their interesting new properties for technological applications [3, 4]. Understanding the growth dynamics and structure of high-quality film during different stages of deposition is the most important prerequisite for its preparation[5]. Throughout the twentieth century, numerous scientists advanced the theory of size-dependent effects in metal thin layers, and various approaches to the problem were proposed. Quantum size effects are decisive for the behavior of isolated metal particles in difficult dimensions (1D and 2D), but both surface and quantum size effects must be considered for ultrathin metal layers [6, 7]. A high nanolayer and/or nanoparticle surface-to-bulk ratio is responsible for these effects. The proportion of surface atoms increases dramatically as the size of nanoparticles decreases; as a result, commonly known physical properties of bulk materials change, such as the density and melting point [8-10]. Electron scattering on phonons, imperfections(occurring in bulk metal) and layer boundaries(present in thin layers responsible for the reduction of their electrical conductivity) affect the properties of metal layers. [11].

Gold is a lustrous, yellow noble metal that does not tarnish, has a face-centered cubic structure, is non-magnetic, melts at 1,336 K, and has a density of 19.320 g cm^{-3} . A small sample of Gold, on the other hand, is quite different, assuming it is small enough: green light is absorbed by 10-nm particles, which causes them to appear red. As the sample size decreases, the melting temperature drops dramatically [12]. Furthermore, gold loses its noble status, and 2- to 3-nm gold nanoparticles are excellent catalysts with high magnetism [7, 13]. Au nanoparticles also become insulators at this size. Thin films of gold are now used in a wide variety of applications, including microelectromechanical and nanoelectromechanical systems [14, 15], sensors, electronic textiles, bioengineering, nonlinear optical property generators or surface-enhanced Raman scattering devices [16], are just a few examples. The film quality is influenced by the structural properties of gold thin films, which can affect the device optical properties and overall capability. At the same time, metal films of various thicknesses are required for various applications, and because these films are polycrystalline, their internal properties and surface roughness can vary greatly from one thickness to another. In this study, the optical and structural properties of gold thin films of various thicknesses are investigated in order to determine the highest value of reflection so as to be used in optical applications.

2. Experimental Part

Firstly, glass substrates were cleaned by propanol for 15 min, then cut into small pieces with a size of $1 \times 1 \text{ cm}^2$, secondly Au thin films were deposited on the cleaned glass substrates using DC- sputtering method by magnetron sputtering machine (Quorum Q150R ES) with a current of 10 mA assisted with Ar gas in a vacuum chamber at room temperature and supplied with magnetic flux which is highest in the center of the cathode region (3350 Gauss), and it decreases as it approaches the edge of the cathode.[17]

the distance between Au target and the sample holder was 2.5 cm for all samples. Deposition time was 9.8, 19.4, and 29.4 min. which provides the film with a thickness of 200, 400, 600 nm, respectively. The thin films thickness was deduced theoretically from the deposition equation [18].

$$D = K I S \quad (1)$$

where D = film thickness (\AA), K = material constant, which is ~ 0.17 for gold in Ar gas, I = sputtering current (mA), S = time (sec.)

To be more accurate in regards to the thickness values, the thickness for one sample of prepared film of 200 nm thickness was tested with a field emission scanning electron microscope (FESEM) (inspect f50 from FEI). This value of thickness was compared with the theoretical one to find the error which may be coming from any steps through the preparation stages. The error ratio was calculated using the following equation[19].

$$D_{\text{calculated}} = D_{\text{experimental}} - D_{\text{theoretical}} / D_{\text{experimental}} * 100 \% \quad (2)$$

Several diagnostics were employed to study the deposited films. Absorption, transmission, and reflection of Au nanoparticles were recorded with UV-1601 spectrophotometer (Shimadzu), Scanning Electron Microscope (SEM) (inspect s50 from FEI) and Energy-Dispersive X-ray (EDX) spectroscope (XFlash 6-10 from Bruker) and X-ray diffractometer (X'Pert PRO from PANalytical). In addition, the dislocation density (δ) and strain of the films (ϵ) were determined, using XRD data, from the following relations [20]:

$$\delta = 1/D_{\text{hkl}}^2 \quad (3)$$

$$\epsilon = \beta \cos\theta/4 \quad (4)$$

using Bragg's formula(Eq.5), the inter planar distance (d) can be calculated[21]:

$$d = n\lambda/2\sin\theta \quad (5)$$

Scherrer formula(Eq.6) was used to calculate the crystal domain size from the full width at half maximum (FWHM) of the peaks:.

$$D = k\lambda/\beta \cos\theta \quad (6)$$

where $k = 0.9$, $\lambda = 1.54$, β is (FWHM), θ is the angle between the incident beam and the reflection lattice planes.

while, the lattice constant (a) was calculated using[20]:

$$a = \lambda/\sin\theta \quad (7)$$

Atomic Force Microscopy (AFM) analysis was done using scanning probe microscope (angstrom advanced AA2000). The AFM was in the contact mode under room temperature.

3. Results and discussion

The calculated thickness value of Au thin film was 204 ± 0.025 nm, according to Equation (2), by considering the values of experimental thickness of 214 and 199.5 nm as shown in Figure 1.

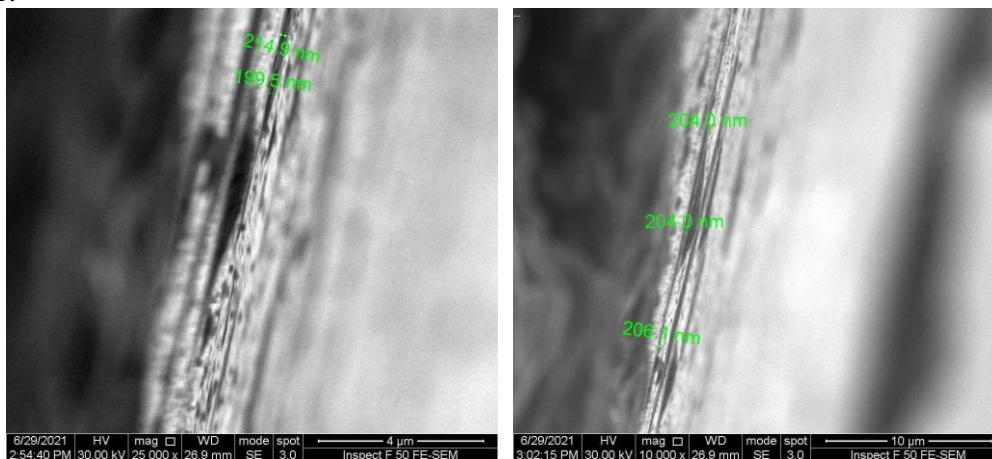


Figure 1- FESEM cross-sectional high-resolution images for Au thin film of 200 nm. Sample

Figure 2 shows the XRD patterns of Au thin films of different thicknesses (200nm, 400nm, and 600nm) prepared on glass substrates by the DC-sputtering method. The diffraction peaks were at planes (111), (200), (220), and (311), which corresponds to $2\Theta = 37, 44, 63,$ and 77 , respectively[22]. The structure is cubic with lattice constant (a) equal to (4.7435) which agrees with JCPDS card no. (00-004-0784). The results indicate that the film thickness is a very important parameter that influences the structural properties since the crystalline size decreased with increasing the thickness, which is attributed to the change of crystallinity and homogeneity of the film with time. In addition, the FWHM, and strain increased with increasing the thickness.

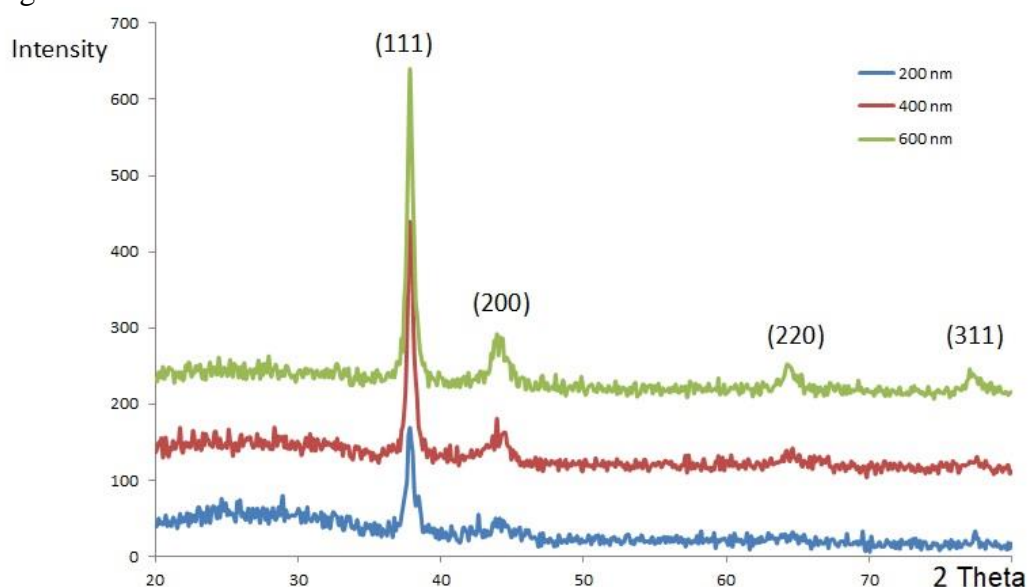


Figure 2-XRD patterns for Au thin films with different thicknesses deposited on glass substrate by the DC-sputtering method.

Crystalline size, FWHM, strain, and dislocation density and other parameters are summarized in Table 1.

Table 1- Crystalline size, FWHM, strain, and dislocation density of Au thin films.

Thickness (nm)	Pos. 2Θ (degree)	hkl	d (nm)	FWHM (β)	D (nm.)	Strain δ	Dislocation density $1/D^2$ ($1/\text{nm}^2$)
200	37.889	111	2.37464	0.3936	33.30	0.0930	9×10^{-4}
	44.1232	200	2.05253	0.9840	13.054	0.2279	58×10^{-4}
	63.0298	220	1.47486	0.4920	24.015	0.1048	17×10^{-4}
	77.4504	311	1.23234	0.2952	36.629	0.0575	7×10^{-4}
400	37.8666	111	2.37601	0.3936	33.30	0.0930	9×10^{-4}
	44.4057	200	2.04013	0.1968	65.204	0.0455	2×10^{-4}
	64.3267	220	1.44822	0.9840	11.923	0.2082	70×10^{-4}
	77.3064	311	1.23428	0.9840	10.999	0.1921	82×10^{-4}
600	37.8698	111	2.37581	0.3936	33.30	0.0930	9×10^{-4}
	43.7510	200	2.06913	0.2952	43.570	0.0684	52×10^{-5}
	64.3542	220	1.44767	0.5904	19.869	0.1249	25×10^{-4}
	77.0639	311	1.23756	0.4920	22.036	0.0962	20×10^{-4}

The comparison between Au thin films of the different thicknesses at the preferred diffraction peak of (111) at $2\theta = 37^\circ$ revealed the change of nanosize of particles, FWHM, strain, and dislocation density [23].

Figure 3 shows the SEM images of Au thin films of different thicknesses (200,400,600 nm) on glass substrates prepared by the DC-sputtering method. As it can be seen that the morphology of the Au surface has improved with the increase of the thickness. This is due to the fact that larger thickness needs more deposition time, which allows the atoms to arrange themselves and thus produce a more homogeneous film[24]. This agrees with the XRD results.

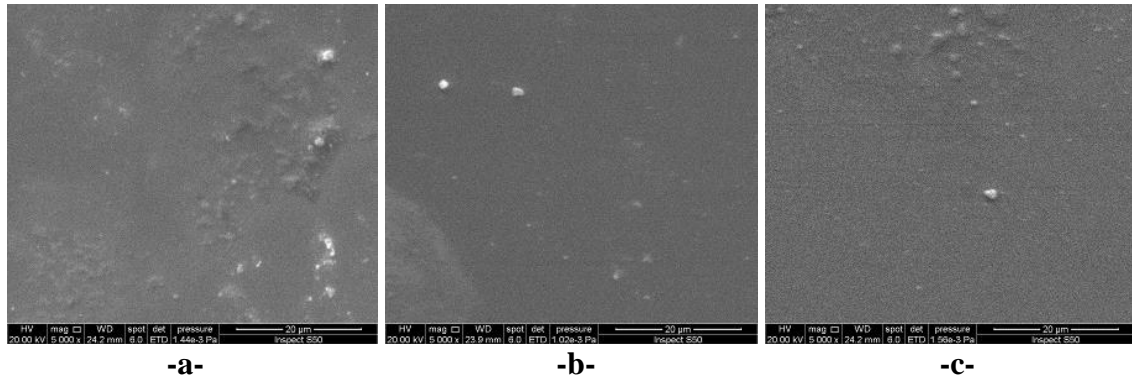


Figure 3-SEM images of Au thin films on glass substrates with thicknesses a- 200 nm, b- 400 nm and c- 600 nm with the same resolution 20 µm.

EDX analysis was performed on the samples with the different thicknesses of 200,400 and 600 nm, and the result showed that the samples have no impurities or contaminations as shown in Figure 4[25].

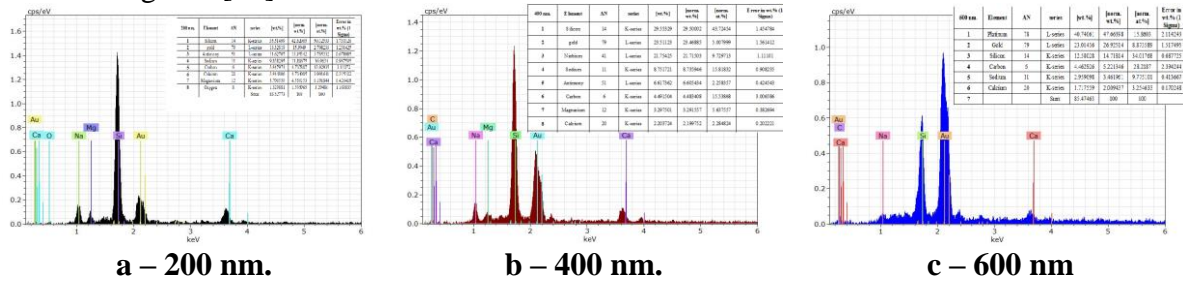


Figure 4- EDX for Au thin films with the various thicknesses inset

Figure 5 shows the topography, in 3D images, for Au thin films surfaces with thicknesses of 200, 400, and 600 nm. Atomic force microscopy (AFM) was also used to perform surface analysis on thin films.

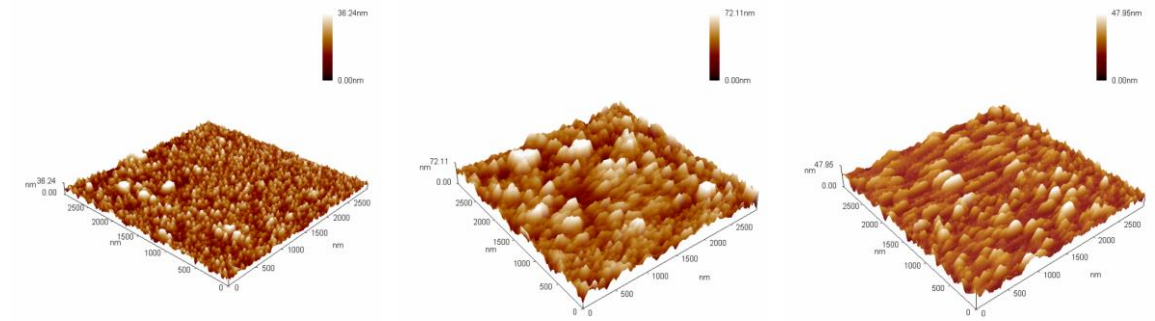


Figure 5-The topography of Au thin films with 200, 400, 600 nm thicknesses.

Figure 6 shows roughness of the Au thin films as a function of thickness. The roughness started to increase at 200nm Au thin film thickness reaching a maximum value of 6.71 at thickness of 400 nm and then decreased to 4.46 at thickness of 600 nm [26, 27]. The behavior of RMS and grain size is the same as that of roughness. AFM results which includes the roughness, RMS, and grain size of Au thin films deposited on glass substrates by the DC-sputtering method are listed in Table 2

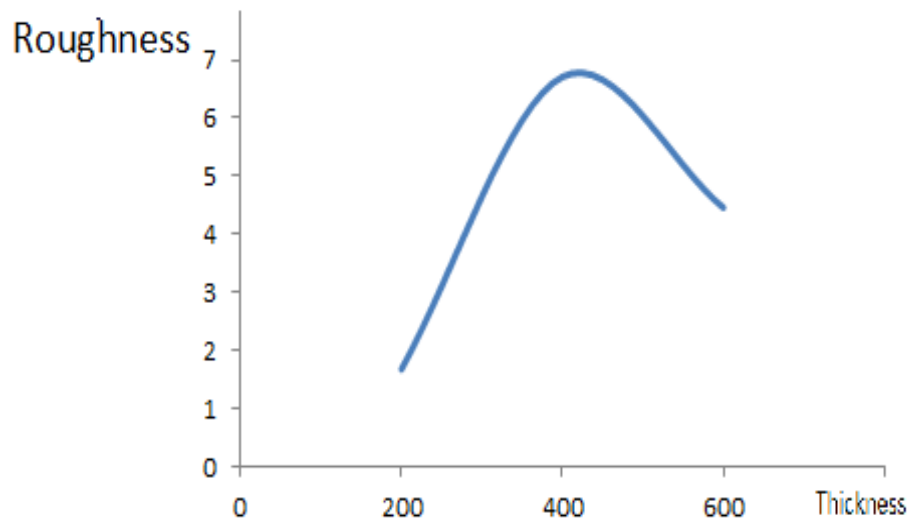


Figure 6- The changes of roughness (nm) of Au thin film with thickness.

Table 2- Roughness, RMS and grain size of Au thin films on glass substrates, data listed from AFM test.

sample	Thickness St (nm)	Roughness Sr (nm)	R M S Sq (nm)	Grain size Sv (nm)
1	200	1.68	2.46	4370.69
2	400	6.71	8.83	7137.17
3	600	4.46	5.74	6779.10

Figure 7 shows the reflection intensity of Au thin film on a glass substrate as a function of wavelength for different thicknesses of 200, 400, and 600 nm. It is indicated that the reflection had a maximum value of 34 at $\lambda \sim 500$ nm for 200 nm thin film thickness. This makes the possibility of using such metal for high reflection applications feasible [28].

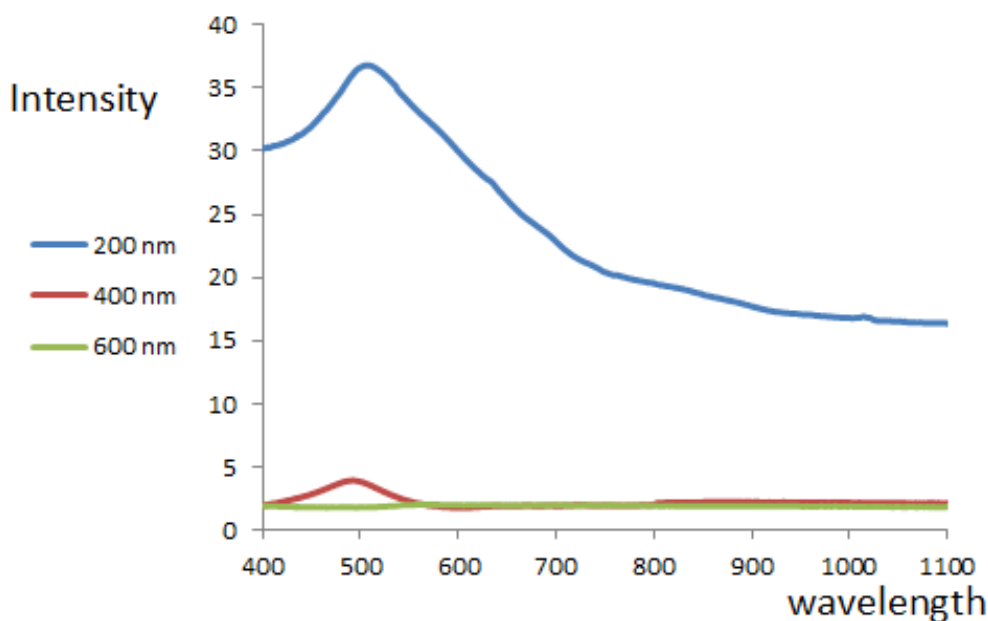


Figure 7- reflection intensity for Au thin films as a function of wavelength for the different thickness (200, 400, and 600 nm).

4. Conclusion

In this paper, the prepared Au thin films were of good quality and the morphology was improved with increasing the film thickness with no impurities or contamination. The results showed that the optimal thickness proved to be 400 nm, which have the highest roughness and RMS. In addition, at 200nm thin film thickness high reflectance value was obtained which makes this metal a good candidate to be used as a resonator for laser applications.

References

- [1] A. Palmero and N. Martin(Eds),2020, "Advanced Strategies in Thin Films Engineering by Magnetron Sputtering," Multidisciplinary Digital Publishing Institute.
- [2] O. O. Abegunde, E. T. Akinlabi, O. P. Oladijo, S. Akinlabi, and A. Ude, "Overview of thin film deposition techniques," *AIMS Materials Science*, vol. 6, no. 2, pp. 174-199, 2019.
- [3] A. Biswas and P. C. Karulkar, "Low cost, tailored polymer-metal nanocomposites for advanced electronic applications," in *2006 16th Biennial University/Government/Industry Microelectronics Symposium*, 2006, pp. 145-149: IEEE.
- [4] A.-P. Hynninen, J. H. Thijssen, E. C. Vermolen, M. Dijkstra, and A. van Blaaderen, "Self-assembly route for photonic crystals with a bandgap in the visible region," *Nature Materials* vol. 6, no. 3, pp. 202-205, 2007.
- [5] Dechun Zhou,Nan Si,Bohong Jiang,Xiufeng Song,Han Huang,Qingmin Ji,Tianchao Niu, "Interfacial effects on the growth of atomically thin film: Group VA elements on Au (111)," *Advanced Materials Interfaces*,vol. 6, no. 21, p. 1901050, 2019.
- [6] C. R. Rao, G. U. Kulkarni, P. J. Thomas, and P. P. Edwards, "Metal nanoparticles and their assemblies,"*Chem. Soc. Rev.*, vol. 29, no. 1, pp. 27-35, 2000.
- [7] E. Roduner, "Size matters:why nanomaterials are different,"*Chem. Soc. Rev.*, vol. 35, no. 7, pp. 583-592, 2006.
- [8] W. Fischer, H. Geiger, P. Rudolf, and P. Wissmann, "Structure investigations on single-crystal gold films," *Applied Physics*, vol. 13, no. 3, pp. 245-253, 1977.
- [9] K. Häupl, M. Lang, P. J. S. Wissmann, and I. Analysis, "X-Ray diffraction investigations on ultra-thin gold films," *surface and interface analysis*, vol. 9, no. 1, pp. 27-30, 1986.

- [10] N. Wang, S. Rokhlin, and D.F. Farson, "Nonhomogeneous surface premelting of Au nanoparticles," *Nanotechnology*, vol. 19, no. 41, p. 415701, 2008.
- [11] K. L. Chopra, "Thin film phenomena," McGraw-Hill Book Company, 1969.
- [12] C. Q. Sun, "Size dependence of nanostructures: Impact of bond order deficiency," *Progress in Solid State Chemistry*, vol. 35, no. 1, pp. 1-159, 2007.
- [13] S. Seino, T. Kinoshita, Y. Otome T. Maki, T. Nakagawa, K. Okitsu, Y. Mizukoshi, T. Nakayama, T. Sekino, K. Niihara, and T.A. Yamamoto, " γ -ray synthesis of composite nanoparticles of noble metals and magnetic iron oxides," *Scripta Materialia*, vol. 51, no. 6, pp. 467-472, 2004.
- [14] S. Nakao, T. Ando, M. Shikida, and K. Sato, "Mechanical properties of a micron-sized SCS film in a high-temperature environment," *J. Micromech. Microeng.*, vol. 16, no. 4, p. 715, 2006.
- [15] F. Liu, P. Rugheimer, E. Mateeva, D. Savage, and M. G. Lagally, "Response of a strained semiconductor structure," *Nature*, vol. 416, no. 6880, pp. 498-498, 2002.
- [16] J. Siegel, O. Lyutakov, V. Rybka, Z. Kolská, and V. Švorčík, "Properties of gold nanostructures sputtered on glass," *Nanoscale Research Letters*, vol. 6, Article no. 96, 2011.
- [17] K. A. Yahya and B. F. Rasheed, "Effect of Electrodes Separation in DC Plasma Sputtering on Morphology of Silver Coated Samples," *Nahrain Journal of Science*, vol. 19, no. 4, pp. 78-85, 2016. 2021). Available: [https://www.mtixtl.com/machine-manual/Plasma%20Sputter %20 Coating.pdf](https://www.mtixtl.com/machine-manual/Plasma%20Sputter%20Coating.pdf)
- [18] D. E. Brewe and B. J. Hamrock, "Simplified solution for elliptical-contact deformation between two elastic solids," *J. of Lubrication Tech.*, vol. 99, no. 4, pp. 485-487, 1977.
- [19] Y. Al-Douri, Q. A. Khasawneh, S. Kiwan, U. Hashim, S.B. Abd Hamid, A.H. Reshak, A. Bouhemadou, M. Ameri, and R. Khenata, "Structural and optical insights to enhance solar cell performance of CdS nanostructures," *Energy Conversion and Management*, vol. 82, pp. 238-243, 2014.
- [20] D. A. S. Mustafa and R. I. M. Al-Rawi, "Structural and Optical Properties for Zn Doped CdO Thin Films Prepared by Pulse Laser deposition," *iraqi journal of science*, vol. 59, no. 2B, pp. 839-846, 2018.
- [21] F. A. Mutlak, M. Jaber, and H. Emad, "Effect of Laser Pulse Energy on the Characteristics of Au Nanoparticles and Applications in medicine," *iraqi journal of science*, vol. 58, no. 4C, pp. 2364-2369, 2017.
- [22] A. A. Khadayeir and W. H. Kareem, "Study the Structural Properties of Au Thin Film Deposited on Poly Vinyl Alcohol Prepared by Plasma Sputtering Method," *Journal of Kufa - Physics* vol. 10, no. 2, pp.105-109, 2018.
- [23] J. Siegel, O. Kvítek, Z. Kolská, P. Slepicka, and V. Švorčík, "Gold nanostructures prepared on solid surface," In Yogiraj Pardhi (Ed.), *Metallurgy - Advances in Materials and Processes*. pp.-4370, 2012. IntechOpen
- [24] N. Azizah, U. Hashim, M.K. Md Arshad, S.C.B. Gopinath, Sh. Nadzirah, M.A. Farehanim, M. F.Fatin, A.K.M. Muaz, A. R. Ruslinda, and R.M. Ayub, "analysis study of single gold nanoparticle system of interdigitated device electrodes (ides) by using energy-dispersive x-ray (EDX)," *ARPJ Journal of Engineering and Applied Sciences*, vol. 11, no. 14, pp. 8889-8892 2016.
- [25] M. Yamamoto, t. Matsumae, Y. Kurashima, H. Takagi, T. Suga, S. Takamatsu, T. Itoh, and E. Higurashi, "Effect of Au film thickness and surface roughness on room-temperature wafer bonding and wafer-scale vacuum sealing by Au-Au surface activated bonding," *Micromachines* vol. 11, no. 5, p. 454, 2020.
- [26] D. I. Yakubovsky, A. V. Arsenin, Y. V. Stebunov, D. Y. Fedyanin, and V. S. Volkov, "Optical constants and structural properties of thin gold films," *Optics Express*, vol. 25, no. 21, pp. 25574-25587, 2017.
- [27] O. Loebich, "The optical properties of gold," *Gold Bull.*, vol. 5, no. 1, pp. 2-10, 1972.